tvst

Article

Paired Optic Nerve Microvasculature and Nailfold Capillary Measurements in Primary Open-Angle Glaucoma

Marissa K. Shoji[1], Clara C. Cousins[1], Chhavi Saini[1], Rafaella Nascimento e Silva[1], Mengyu Wang[1], Stacey C. Brauner[1], Scott H. Greenstein[1], Louis R. Pasquale[2], and Lucy Q. Shen[1]

[1] Department of Ophthalmology, Massachusetts Eye and Ear, Harvard Medical School, Boston, MA, USA
[2] Department of Ophthalmology, Icahn School of Medicine at Mount Sinai, New York, NY, USA

Correspondence: Lucy Q. Shen, Massachusetts Eye and Ear, 243 Charles Street, Boston, MA 02114, USA. e-mail: lucy_shen@meei.harvard.edu

Received: February 8, 2021
Accepted: April 19, 2021
Published: June 10, 2021

Keywords: glaucoma; optic coherence tomography angiography; nailfold capillaroscopy; microvascular pathology

Citation: Shoji MK, Cousins CC, Saini C, Nascimento e Silva R, Wang M, Brauner SC, Greenstein SH, Pasquale LR, Shen LQ. Paired optic nerve microvasculature and nailfold capillary measurements in primary open-angle glaucoma. Transl Vis Sci Technol. 2021;10(7):13, https://doi.org/10.1167/tvst.10.7.13

Purpose: To assess microvascular beds in the optic nerve head (ONH), peripapillary tissue, and the nailfold in patients with primary open-angle glaucoma (POAG) versus controls.

Methods: Patients with POAG (n = 22) and controls (n = 12) underwent swept-source optical coherence tomography angiography of ophthalmic microvasculature and nailfold video capillaroscopy of the hand. The main outcomes were vessel density (VD) and blood flow of the ONH, the peripapillary and the nailfold microvasculatures.

Results: Patients with POAG were younger than controls (63.5 ± 9.4 vs. 69.9 ± 6.5 years, $P = 0.03$). Deep ONH VD and blood flow were lower in patients with POAG than controls (39.1% ± 3.5% vs. 43.8% ± 5.7%; 37.8% ± 5.3% vs. 46.0% ± 7.8%, respectively, $P < 0.02$ for both); similar results were observed with peripapillary VD (37.9 ± 2.6%, 43.4 ± 7.6%, respectively, $P = 0.03$). Nailfold capillary density and blood flow were lower in patients with POAG than controls (8.8 ± 1.0 vs. 9.8 ± 0.9 capillaries/mm; 19.9 ± 9.4 vs. 33.7 ± 9.8 pL/s, respectively; $P < 0.009$ for both). After adjusting for age and gender, deep ONH VD and blood flow, peripapillary VD, and nailfold capillary blood flow were lower in POAG than controls ($\beta = -0.04, -0.07, -0.05, -13.19$, respectively, $P \leq 0.046$ for all). Among all participants, there were positive correlations between deep ONH and nailfold capillary blood flow (Pearson's correlation coefficient $r = 0.42$, $P = 0.02$), peripapillary and nailfold capillary density ($r = 0.43$, $P = 0.03$), and peripapillary and nailfold capillary blood flow ($r = 0.49$, $P = 0.01$).

Conclusions: Patients with POAG demonstrated morphologic and hemodynamic alterations in both ophthalmic and nailfold microvascular beds compared to controls.

Translational Relevance: The concomitant abnormalities in nailfold capillaries and relevant ocular vascular beds in POAG suggest that the microvasculature may be a target for POAG treatment.

Introduction

Primary open-angle glaucoma (POAG) is characterized by loss of retinal ganglion cells and their axons, and it exhibits manifestations of vascular pathology.[1–4] Hemodynamic dysfunction is present in ocular and systemic vasculature in POAG when compared to patients without glaucoma.[5–7]

Color Doppler imaging and laser Doppler flowmetry studies have established decreased systolic and diastolic blood flow velocities in ocular blood vessels and altered retinal blood flow in patients with POAG, but these modalities fail to assess blood flow in precapillary arterioles or in capillaries.[8–14] More recently, studies utilizing optical coherence tomography angiography (OCTA), a noninvasive and high-resolution imaging method, demonstrated decreased vessel density of the optic nerve head (ONH) and peripapillary microvasculature in patients with POAG.[15–18] Swept-source OCTA (SS-OCTA) achieves deep tissue penetration with a low signal-to-noise ratio,[19] while

a blood flow detection algorithm known as OCTA Ratio Analysis algorithm (OCTARA) has improved detection sensitivity of low blood flow and reduced motion artifacts.[20] Scaled relative OCTARA value correlates with blood flow, and we have previously measured the integrated OCTARA signal (IOS) to show alteration in ONH and peripapillary microvascular blood flow in patients with POAG compared to control participants.[21,22]

For evaluation of the systemic microcirculation, the nailfold capillaries provide an accessible nonocular vascular bed to visualize and quantify blood flow and velocity, as the orientation of these capillaries is parallel to the skin.[23] Additionally, the nailfold capillaries exhibit morphologic features similar to ophthalmic vascular beds; namely, the closed vascular loops with hairpin turns in the nailfold capillaries resemble the hairpin turns of vessels at the junction of the ONH and retina.[24] Gasser and Flammer[25] were first to describe morphologic alterations in nailfold capillaries by means of nailfold microscopy in patients with POAG; subsequently, we and others have confirmed their findings.[26,27]

Although the relationship between ophthalmic and finger blood flow has been explored before,[28,29] the availability of SS-OCTA and nailfold capillary microscopy allow for quantitative measurements of both microvascular beds in the same patients. Studying these microvascular systems together may ultimately lead to the consensus that systemic microvascular pathology exists in POAG and motivate the development of systemic treatment that reverses these alterations. Therefore, this study aimed to evaluate the microvascular parameters of the optic nerve and finger nailfold in the same individuals and compare the measurements in POAG to control participants. Furthermore, we explored potential correlations between ophthalmic microvasculature and nailfold capillary measurements in our study participants.

Methods

Study Design

This cross-sectional, observational study was approved by the Massachusetts Eye and Ear (MEE) Institutional Review Board and adhered to the tenets of the Declaration of Helsinki. Patients with POAG and control participants aged 35 to 80 years were recruited from the glaucoma service and the comprehensive ophthalmology service, respectively, at MEE (Boston, MA, USA) between July 2014 and December 2018. Written informed consent was obtained from all participants.

Inclusion criteria for all participants were visual acuity of at least 20/40 and refractive error between −6 diopters (D) and +6D. In all participants, exclusion criteria were significant retinal or optic nerve disease other than glaucoma causing visual field loss, optic disc torsion more than 15°,[30] tilt ratio >1.3 (maximum to minimum optic disc diameter),[31] and history of connective tissue disorders, as they have been associated with nailfold capillary changes in previous studies.[32]

Additional inclusion criteria for patients with POAG were open angles on gonioscopy, glaucomatous visual field loss confirmed on the subsequent visual field test, and corresponding glaucomatous optic nerve damage evidenced by one or more red sectors on an optical coherence tomography (OCT) sector image, which was reviewed to ensure that there was abnormal thinning of the retinal nerve fiber layer (RNFL) and no significant artifacts. Patients with secondary open-angle glaucoma; unreliable visual field test results (Humphrey Visual Field [HVF] perimeter; Carl Zeiss Meditec, Dublin, CA, USA), defined as fixation loss >33%, false-positive rate >20%, and false-negative rate >20%; or a history of penetrating glaucoma surgeries, such as trabeculectomy and tube shunt surgery, were excluded.

Additional inclusion criteria for control participants were a negative family history of glaucoma, intraocular pressure (IOP) measurements ≤21 mm Hg, cup-disc ratio (CDR) ≤0.6, and CDR asymmetry between eyes <0.2. These criteria were established from prior OCTA and nailfold capillary studies.[21,33]

Image Acquisition and Processing

All participants underwent ocular posterior segment imaging and imaging of peripheral digit capillaries: imaging of the optic nerve head and peripapillary region using SS-OCTA and spectral-domain OCT (SD-OCT), as well as imaging of the nailfold capillaries of the nondominant hand using a nailfold video capillaroscope. Same-day imaging of both microvascular systems was encouraged but not required in this study due to logistical challenges, such as the length of time for each imaging test and the waiting time between the two tests (over 60 minutes). When the two imaging tests were not performed on the same day, the time between nailfold and OCTA imaging was calculated with the visit for nailfold imaging as time zero; OCTA imaging conducted after nailfold imaging yielded a positive duration while OCTA imaging before nailfold imaging yielded a

negative duration. The participant's blood pressure and heart rate were also measured at the time of nailfold imaging.

OCT Angiography and Structural OCT Measurements

The ONH and peripapillary region of both eyes were imaged after pharmacologic pupil dilation by utilizing the SS-OCT device (Triton; Topcon, Tokyo, Japan) to obtain 3-mm × 3-mm and 4.5-mm × 4.5-mm OCT and OCTA scans centered on the ONH. The Triton SS-OCT uses a 1050-nm wavelength light source, which allows for deep signal penetration through the prelaminar and laminar tissue of the optic nerve to provide analysis of both superficial and deep vasculature.[20] Patients underwent RNFL imaging with SD-OCT (Spectralis; Heidelberg Engineering GmbH, Heidelberg, Germany) during the same visit, as this measurement was not available on the SS-OCT device at the time of the study. Average peripapillary RNFL thickness was obtained automatically from SD-OCT scans.

For OCTA imaging analysis, one eye per participant was included in the study. The eye with the worse HVF mean deviation (MD) was selected in patients with POAG, and one eye was randomly selected for control participants. Eyes were excluded if significant motion artifacts were present on OCTA or if the OCTA image quality score was below 40.[34]

OCTA images were processed based on a previously published protocol.[21] Briefly, for ONH microvasculature analysis, the en face OCTA image from the 3-mm × 3-mm scan was used. A superficial angiogram was generated from the internal limiting membrane to Bruch's membrane (Fig. 1D), while the deep angiogram was generated from Bruch's membrane to 390 µm below Bruch's membrane (Fig. 1E). For the peripapillary microvasculature, an angiogram was generated from the internal limiting membrane to the interface of the RNFL with the ganglion cell layer from the 4.5-mm × 4.5-mm scans (Fig. 1F).[35,36]

SS-OCTA images along with structural OCT scans obtained by SS-OCT (320 horizontal scans per eye) were imported into ImageJ (Fiji) software (ImageJ; National Institutes of Health, Bethesda, MD, USA) and analyzed by two independent readers (MKS, RNS) who were masked to diagnosis. Using a customized ImageJ plugin, the ONH margin was generated by manually marking the termination of Bruch's membrane on structural OCT cross-sectional images, spaced 47 µm apart.[21] The ONH margin was then superimposed on the corresponding OCTA angiograms to define the ONH area (Figs. 1G, 1H). The peripapillary region was a 0.70-mm-wide elliptical annulus extending radially from the ONH margin

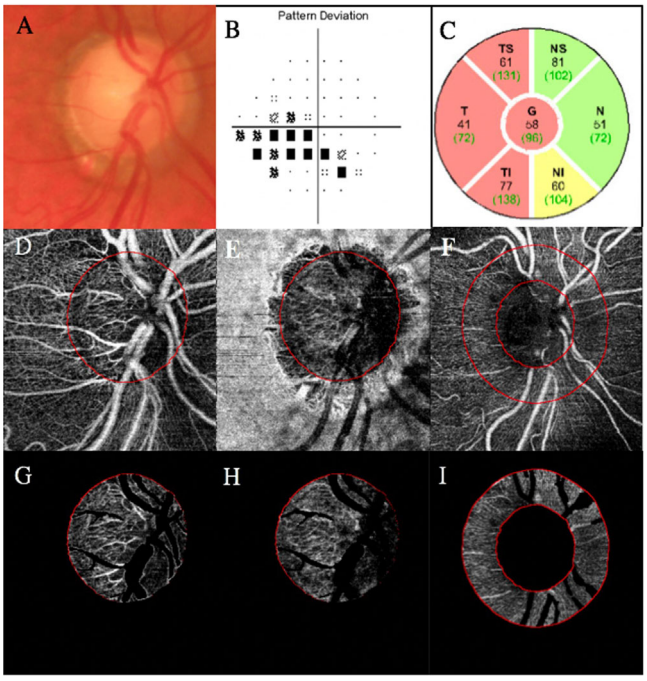

Figure 1. The disc photo of the right eye from a patient with POAG (A), HVF pattern deviation plot (B), and RNFL thickness sectors (C) are displayed. The superficial ONH angiogram (D) was generated from the 3-mm × 3-mm en face image from the internal limiting membrane (ILM) to Bruch's membrane (BM). The deep ONH layer (E) was from BM to 390 µm below BM. *Red markings* delineate the ONH margin based on BM opening. The peripapillary region OCTA (F) was generated from the 4.5-mm × 4.5-mm en face angiogram from the ILM to the interface of the RNFL with the ganglion cell layer. *Red markings* delineate an annulus of 0.70 mm in width from BM opening. Large vessels are manually excluded from the superficial ONH angiogram (G) and superimposed on the deep ONH angiogram (H) to limit projection artifact. The large vessels of the peripapillary region are automatically excluded (I). In this example, the measurement for deep ONH VD was 35.0%, and IOS was 38.8% (H). The peripapillary VD was 35.1%, and IOS was 39.0% (I).

(Figs. 1F, 1I).[15,17,21] To avoid projection artifacts, areas occupied by large vessels were excluded from OCTA images of the ONH by manual selection of large vessels in the en face superficial ONH angiogram, and the same areas were excluded for the deep angiogram. Large vessels in the peripapillary region were automatically excluded using customized ImageJ software plugins, which use a local thresholding algorithm to identify large vessels based on intensity and contrast information.[21] This was performed for both patients with POAG (Fig. 1) and control participants (Supplementary Fig. S1).

After large vessel removal, we measured OCTA parameters of the deep ONH and superficial peripapillary region, as we and others have described pathology in these microvascular beds in patients with POAG.[21,35] Vessel density (VD) was defined as the percentage of

area occupied by the microvasculature within the area of interest after excluding the area occupied by large blood vessels. IOS, which is suggestive of flow, was calculated as the mean grayscale value of the en face OCTA image in the area of interest divided by constant maximum pixel intensity and displayed as a percentage.[21]

Nailfold Capillaroscopy

Nailfold capillaroscopy was performed with a BK-XW880 nailfold video capillaroscope (Biobase Meihua Trading, Jinan, Shandong, China) at 300× magnification to image capillaries from the fourth and fifth digits of the nondominant hand of each participant. The fourth and fifth digits on the nondominant hand were chosen since they have higher skin transparency and are less likely to experience inadvertent microtraumas from daily activity compared with digits from the dominant hand.[23,37] Cedarwood oil was applied to the nailfold to facilitate visualization under the microscope. Imaging was initiated at the lateral aspect of the nailfold, moving medially, covering the entire nailfold. Capillary density, calculated as the number of distal row capillaries in a 1-mm span in each digit, was assessed by two independent readers (MKS, CCC) masked to diagnosis.[23,38,39] The "90-degree rule" was used to define the distal row of the capillary bed as containing only the capillaries for which the angle between the apex of that capillary and the apices of its two adjacent capillaries is greater than 90 degrees[38,39] (Figs. 2A, 2D). Capillary density at the first, midpoint, and last video frames was averaged to generate the measurement.

Nailfold capillary blood flow imaging was acquired as a video for the first five capillaries for 10 seconds on each capillary. The measurement was performed by two independent readers (MKS, CCC) masked to diagnosis, consistent with prior protocols.[33,40] Nailfold videos were converted to image sequences and imported into ImageJ. Blood speed was calculated by dividing the distance of the first visible void in the blood column in each capillary, which was tracked between consecutive frames (Figs. 2B, 2C, 2E, 2F), by the time elapsed between a consecutive set of frames (25 frames/s). The diameter of the capillary in the region of blood column void movement was also measured and used to calculate the cross-sectional area of the vessel lumen and subsequently capillary blood flow as picoliters per second (pL/s).

Statistical Analysis

Statistical analysis was conducted using R Language Platform (Version 3.4.3; R Foundation, Vienna, Austria). Interreader reproducibility was measured through intraclass correlation coefficients (ICCs) for all OCTA and nailfold measurements. The mean values of measurements by both readers were used for analyses. Two-tailed Student's *t*-test was used to test group differences for continuous variables, and Fisher's exact test was used to compare differences in frequencies of categorical variables between groups. Multiple linear regression analyses were performed with OCTA and nailfold metrics as dependent variables to assess the difference between POAG and controls while accounting for age and gender as covariates; controls served as the reference group. Multiple linear regression was applied to assess the partial Pearson's correlations between nailfold and OCTA measurements among all participants and was adjusted for age and the time between two imaging visits. In the POAG group, partial Pearson's correlations between the same metrics were obtained while adjusting for HVF MD and the time between two imaging visits. *P* value correction

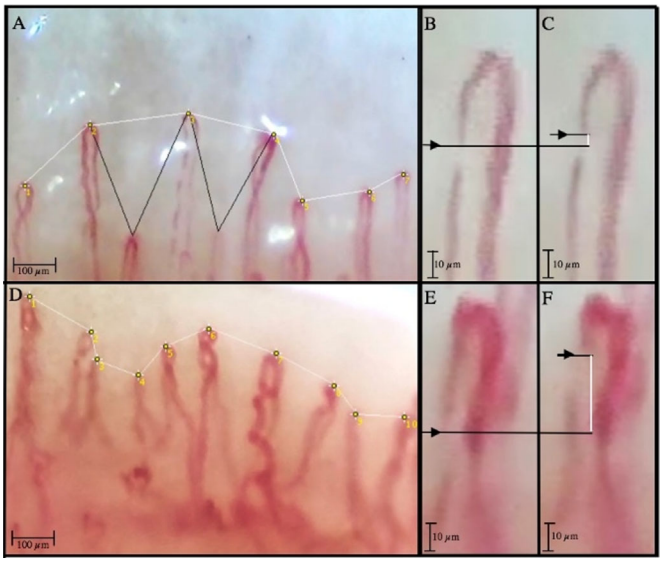

Figure 2. (A–C) Nailfold capillary analysis of a patient with POAG whose ophthalmic microvasculature is shown in Figure 1. Nailfold capillary density (A) is the number of distal row capillaries averaged over the first, midpoint, and last video frames (8.9 capillaries/mm for this example). A distal row capillary is defined as one with its apex in the row closest to the finger nail plate such that an angle greater than 90° is created between the apex of that capillary and the apices of its two adjacent capillaries. The *white lines* link capillaries in the distal row (seven in this video frame) while the vertices at the *black angles* indicate capillaries not in the distal row. Nailfold capillary flow (11.0 pL/s in this example) was calculated by tracking a gap in the blood column indicated as a *white line* between sequential frames 0.25 seconds apart (B, C). (D–F) Corresponding capillary density (9.8 capillaries/mm for this example with 10 capillaries in the video frame) and blood flow (39.2 pL/s) measurements in the control participant whose ophthalmic microvasculature is shown in Supplementary Figure S1.

for multiple comparisons by the false discovery rate (FDR) method was applied for both univariable and multivariable analysis, and FDR-corrected $P < 0.05$ was considered significant.[41]

Results

Forty-four participants (30 POAG and 14 controls) were recruited and underwent OCTA of the ophthalmic microvasculature and nailfold capillary imaging. Six participants (14.3%) were excluded due to poor OCTA quality and motion artifact, and four participants (9.1%) were excluded due to poor quality of nailfold capillary imaging. Therefore, 22 patients with POAG and 12 controls were entered into the analysis. Patients with POAG were younger (63.5 ± 9.4 years) than control participants (69.9 ± 6.5 years, $P = 0.03$) but were similar in gender (45.5% vs. 33.3% male, $P = 0.72$) and ethnicity (86.4% vs. 91.7% Caucasian, $P > 0.99$, Table 1). For patients with POAG, the average HVF MD and pattern standard deviation of the worse eye were −3.4 ± 2.8 dB and 5.7 ± 4.0

Table 1. Baseline Characteristics of the Study Population

Characteristic	POAG (n = 22)	Controls (n = 12)	*P* Value
Participants			
Gender, male (%)	45.5	33.3	0.72
Age (years)	63.5 ± 9.4	69.9 ± 6.5	**0.03**
Ethnicity, Caucasian (%)	86.4	91.7	>0.99
Systemic findings			
Systolic blood pressure (mm Hg)[a]	130.9 ± 21.1	128.9 ± 14.2	0.78
Diastolic blood pressure (mm Hg)[a]	77.2 ± 14.1	76.8 ± 10.0	0.94
Mean arterial pressure (mm Hg)[a]	95.1 ± 16.1	94.2 ± 10.2	0.86
Heart rate[b]	65.0 ± 10.5	68.9 ± 10.0	0.40
Ophthalmologic findings			
Cup/disc ratio	0.74 ± 0.08	0.31 ± 0.08	**<0.0001**
IOP (mm Hg)	13.1 ± 2.8	15.5 ± 1.9	**0.007**
Maximum IOP (mm Hg)	20.2 ± 3.3	NA	NA
HVF MD (dB)	−3.4 ± 2.8	NA	NA
HVF PSD (dB)	5.7 ± 4.0	NA	NA
Average RNFL thickness (µm)	71.3 ± 14.0	94.2 ± 10.7	**<0.0001**
Systemic conditions			
Diabetes mellitus (%)	0	16.7	0.12
History of smoking (%)	31.8	33.3	>0.99
Systemic hypertension (%)	36.3	41.7	>0.99
BMI (kg/m^2)	24.4 ± 4.9	26.6 ± 5.6	0.30
Migraine (%)	27.2	25.0	>0.99
Medication usage			
Systemic antihypertensives (%)	36.3	41.7	>0.99
Average number of antihypertensives	0.4 ± 0.6	0.6 ± 0.8	0.47
Duration of antihypertensives >1 year (%)	87.5	60.0	0.51
Systemic blood thinners (%)	40.9	66.7	0.28
Number of glaucoma medications	1.5 ± 0.9	NA	NA
Time between			
OCTA and nailfold imaging (years)	1.1 ± 1.1	0.8 ± 1.2	0.54

Data are expressed as mean ± standard deviation unless otherwise specified.

Systemic findings were obtained at the same time as nailfold capillary imaging. Other information was obtained from the ophthalmology clinic visit closest to the OCTA imaging date.

Bold font indicates $P < 0.05$. BMI, body mass index; NA, not applicable.

[a]Available for 86.3% of patients with POAG and 91.7% controls.

[b]Available for 68.1% of patients with POAG and 66.7% controls.

Table 2. Comparison of Ophthalmic Microvascular Measurements and Nailfold Capillary Metrics Between POAG and Control Participants

Measurement	POAG	Controls	*P* Value
OCTA vessel density			
Deep optic nerve head (%)	39.1 ± 3.5	43.8 ± 5.7	**0.02**
Peripapillary (%)	37.9 ± 2.6	43.4 ± 7.6	**0.03**
OCTA IOS			
Deep optic nerve head (%)	37.8 ± 5.3	46.0 ± 7.8	**0.005**
Peripapillary (%)	44.1 ± 3.1	46.8 ± 3.9	0.052
Nailfold capillary metrics			
Nailfold capillary density (capillaries/mm)	8.8 ± 1.0	9.8 ± 0.9	**0.009**
Nailfold capillary blood flow (pL/s)[a]	19.9 ± 9.4	33.7 ± 9.8	**0.0007**

Data are expressed as mean ± standard deviation unless otherwise specified.
IOS is a surrogate marker of flow. Bold font indicates FDR-corrected $P < 0.05$.
[a]One POAG participant was excluded from the nailfold capillary blood flow measurement due to video quality.

dB, respectively. CDR differed significantly between POAG (0.74 ± 0.08) and control participants (0.31 ± 0.08, $P < 0.0001$), as did the average RNFL thickness (71.3 ± 14.0 µm vs. 94.2 ± 10.7 µm, $P < 0.0001$). IOP at the clinic visit closest to OCTA imaging was significantly lower in patients with POAG compared to controls (13.1 ± 2.8 mm Hg vs. 15.5 ± 1.9 mm Hg, $P = 0.007$). Nineteen of 22 patients with POAG (86.3%) were medically managed with an average of 1.5 ± 0.9 glaucoma medications per patient. The remaining 3 of 22 (13.7%) patients with POAG had undergone selective laser trabeculoplasty.

The POAG and control groups did not differ in the prevalence of systemic conditions such as diabetes mellitus, systemic hypertension, smoking history, and migraine ($P \geq 0.12$ for all, Table 1). They did not differ in systemic blood pressure, heart rate, number and duration of antihypertensive medications, and use of systemic blood thinner medications ($P \geq 0.28$ for all). They also had similar body mass index (24.4 ± 4.9 kg/m^2 vs. 26.6 ± 5.6 kg/m^2, $P = 0.30$). OCTA imaging and nailfold capillary imaging were performed on the same day in eight patients with POAG (36.4%) and seven controls (58.3%, $P = 0.29$), while other study participants preferred to have the two imaging tests done on separate days. Nailfold imaging was done before OCTA for most participants, except for three patients with POAG (13.6%). For those participants who were not imaged on the same day, nailfold imaging was performed 23.0 ± 13.6 months before OCTA for 5 control participants and 21.5 ± 11.1 months before OCTA for 11 patients with POAG and 12.0 ± 7.0 months after OCTA for 3 patients with POAG. Overall, the difference in the mean time between OCTA and nailfold imaging was not statistically significant between patients with POAG and controls (1.1 ± 1.1 vs. 0.8 ± 1.2 years, $P = 0.54$).

For OCTA parameters, the ICCs were >0.98 for all parameters (Supplementary Table S1). Patients with POAG had decreased deep ONH VD (39.1% ± 3.5%) compared to controls (43.8% ± 5.7%, $P = 0.02$), as well as decreased VD in the peripapillary region (37.9% ± 2.6% vs. 43.4% ± 7.6%, $P = 0.03$, Fig. 1, Table 2). The IOS, a surrogate for flow, of the deep ONH was significantly lower in patients with POAG compared to control participants (37.8% ± 5.3% vs. 46.0% ± 7.8%, $P = 0.005$). The difference in peripapillary IOS between patients with POAG (44.1% ± 3.1%) and control participants (46.8% ± 3.9%, $P = 0.052$) was borderline significant.

For nailfold capillary measurements, the ICCs were >0.81 for all measurements (Supplementary Table S1). Patients with POAG had significantly lower nailfold capillary density (8.8 ± 1.0 capillaries/mm) compared to control participants (9.8 ± 0.9 capillaries/mm, $P = 0.009$, Fig. 2, Table 2). Patients with POAG had significantly lower nailfold capillary blood flow compared to control participants (19.9 ± 9.4 pL/s vs. 33.7 ± 9.8 pL/s, $P = 0.0007$).

Multiple linear regression was performed to evaluate the difference in OCTA and nailfold measurements between POAG and control groups after adjusting for the effects of age and gender. Deep ONH vessel density was 4% lower, where percentage was the unit for OCTA measurements (95% confidence interval [CI], −7% to −0.2%, $P = 0.046$), peripapillary vessel density was 5% lower (95% CI, −9% to −1%, $P = 0.02$), and deep ONH IOS was 7% lower (95% CI, −12% to −3%, $P = 0.008$) in patients with POAG compared to controls after adjusting for age and gender ($P \geq$

Table 3. Multiple Linear Regression Comparing Ophthalmic Microvascular Measurements Between POAG and Control Participants

Variable	β	95% CI		*P* Value
		Lower Bound	Upper Bound	
Deep ONH OCTA vessel density (%)				
Group difference	−0.04	−0.07	−0.002	**0.046**
Covariate age	0.001	−0.0008	0.003	0.50
Covariate sex (reference male)	−0.03	−0.06	0.0003	0.12
Peripapillary OCTA vessel density (%)				
Group difference	−0.05	−0.09	−0.01	**0.02**
Covariate age	−0.0001	−0.002	0.002	0.93
Covariate sex (reference male)	−0.02	−0.06	0.02	0.35
Deep ONH OCTA IOS (%)				
Group difference	−0.07	−0.12	−0.03	**0.008**
Covariate age	0.0003	−0.002	0.003	0.82
Covariate sex (reference male)	−0.05	−0.09	−0.002	0.10
Peripapillary OCTA IOS (%)				
Group difference	−0.02	−0.05	0.003	0.09
Covariate age	0.0003	−0.001	0.002	0.82
Covariate sex (reference male)	−0.008	−0.03	0.02	0.53

For all comparisons, control group served as the reference.
IOS is a surrogate marker of flow.
Bold font indicates FDR-corrected for multiple comparisons $P < 0.05$.

Table 4. Multiple Linear Regression Comparing Nailfold Capillary Metrics Between POAG and Control Participants

Variable	β	95% CI		*P* Value
		Lower Bound	Upper Bound	
Nailfold capillary density (capillaries/mm)				
Group difference	−0.80	−1.59	−0.02	0.05
Covariate age	0.02	−0.02	0.06	0.68
Covariate sex (reference male)	−0.13	−0.89	0.62	0.93
Nailfold capillary blood flow (pL/s)				
Group difference	−13.19	−20.86	−5.54	**0.004**
Covariate age	0.09	−0.35	0.54	0.78
Covariate sex (reference male)	0.33	−7.29	7.96	0.93

For all comparisons, control group served as the reference.
Bold font indicates FDR-corrected for multiple comparisons $P < 0.05$.

0.10, Table 3). Similarly, nailfold capillary blood flow was 13.19 pL/s lower (95% CI, −20.86 to −5.54 pL/s, $P = 0.004$) in POAG participants compared to controls after adjusting for the same covariates ($P \geq 0.78$, Table 4), while the difference in nailfold capillary density was borderline significant ($\beta = -0.80$ capillaries/mm; 95% CI, −1.59 to −0.02 capillaries/mm, $P = 0.05$).

The correlations between ophthalmic and nailfold capillary measurements were assessed after adjusting for age, which was different between the POAG and control groups, and for the time between nailfold capillary and OCTA imaging visits. Nailfold capillary density correlated positively with peripapillary vessel density among all participants (Pearson's correlation coefficient $r = 0.43$, $P = 0.03$) but not with deep ONH vessel density ($r = 0.01$, $P = 0.98$, Fig. 3). Nailfold capillary blood flow correlated positively with peripapillary IOS, which is the OCTA parameter suggestive of flow, among all participants ($r = 0.49$, $P = 0.01$); nailfold capillary blood flow also correlated positively with deep ONH IOS ($r = 0.42$,

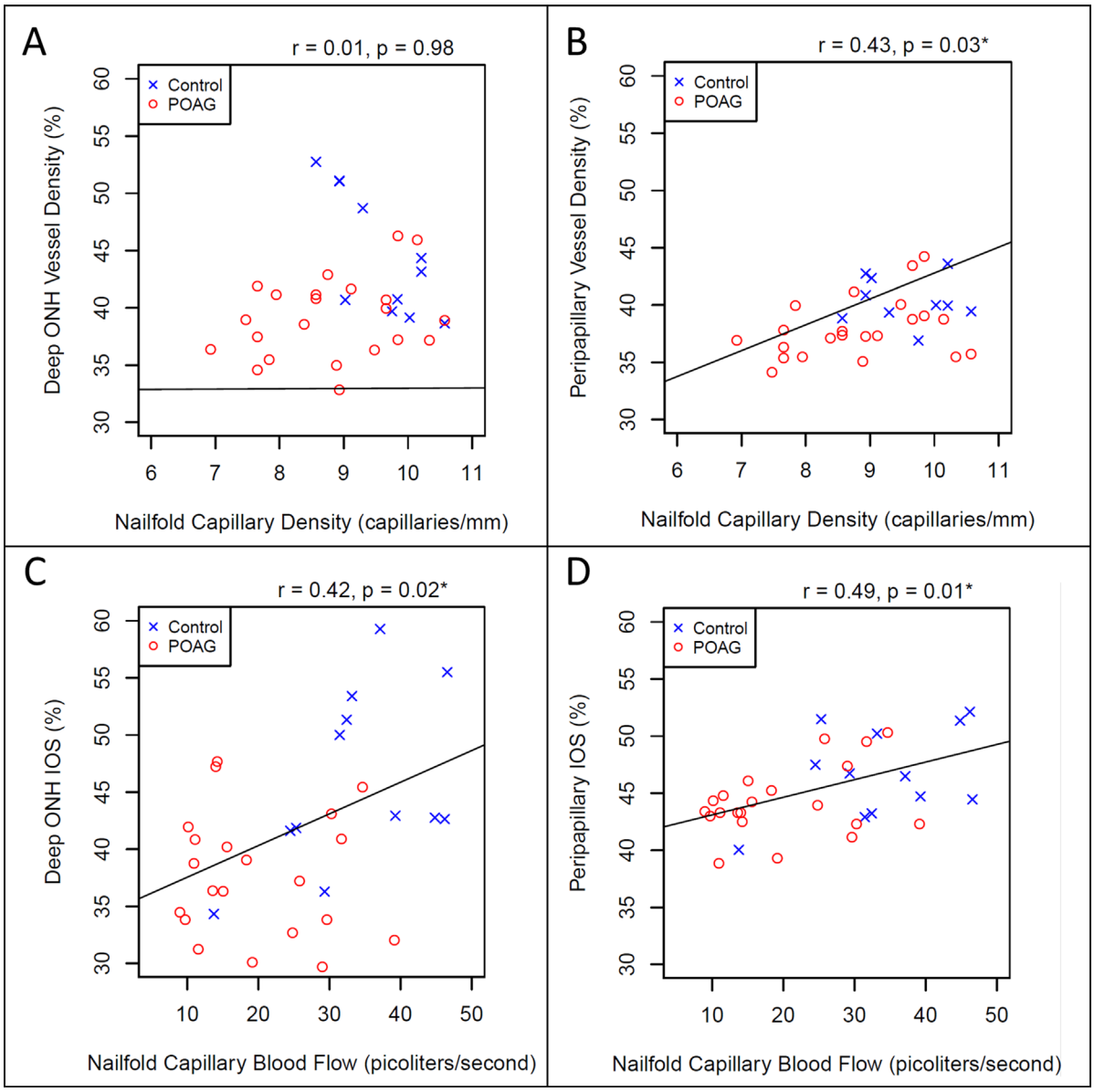

Figure 3. The *top row* displays the correlation of nailfold capillary density with deep ONH vessel density (A) and peripapillary vessel density (B). The *bottom row* depicts the correlation of nailfold capillary blood flow with deep ONH IOS (C), a surrogate marker of flow, and peripapillary IOS (D). POAG patient data are indicated by *red circles* and control data are represented by *blue crosses*. In all graphs, Pearson's correlation coefficient (*r*) and the *P* value are displayed and the *black regression line* is the slope adjusted for age and time between imaging visits. Significant correlations are found between nailfold capillary density and peripapillary vessel density (B), nailfold capillary blood flow and deep ONH IOS (C), and nailfold capillary blood flow and peripapillary IOS (D). *Statistically significant difference, $P < 0.05$.

$P = 0.02$). The correlations between OCTA and nailfold capillary measurements were also assessed in the POAG group. There were no statistically significant correlations between nailfold capillary and OCTA measurements (Supplementary Table S2), even after adjusting for HVF MD, which had been reported to correlate with OCTA measurements by others,[42,43] and for the time between two imaging visits (Supplementary Fig. S2).

Discussion

This study demonstrates concomitant abnormalities in ophthalmic microvasculature and nailfold capillaries in patients with POAG. Specifically, both vessel density and flow in the ophthalmic and systemic microvasculature were reduced in the same group of patients with POAG compared to controls. This

study confirms previous studies, provides quantitative evidence showing the systemic vascular pathology in POAG, and establishes the microvasculature as a potential treatment target for POAG.

The compromise in ophthalmic microvasculature was demonstrated by low VD in the deep ONH layer and peripapillary region, as well as low flow (IOS) in the deep ONH layer in patients with POAG. Our method of OCTA analysis used an anatomic landmark, Bruch's membrane opening, to clearly define the ONH region, as well as removed signals and shadowing artifacts from large vessels to isolate the microvasculature and optimize analysis. Our findings are supported by our previous study and others that have demonstrated similar localization of ophthalmic microvasculature abnormalities in the deep ONH and peripapillary regions using OCTA in patients with POAG.[15,17,18,21] The deep ONH layer extends from Bruch's membrane to 390 µm below Bruch's membrane and contains the laminar region; thus, microvasculature of this region likely involves branches of the short posterior ciliary arteries.[44,45] The peripapillary region is thought to be supplied by the circle of Zinn from the short posterior ciliary arteries. The alterations in the microvascular systems in both the deep ONH and peripapillary region in patients with POAG suggest that these branches originating from short posterior ciliary arteries may play a role in the vascular pathology of POAG. This was supported by previous studies utilizing color Doppler imaging to demonstrate hemodynamic compromise in the short posterior ciliary arteries in patients with POAG compared to controls.[46,47]

In the same participants, we also showed that POAG had significantly decreased nailfold capillary blood flow compared to control participants. Our results are based on reproducible capillary density measurement techniques, such as the 90-degree rule,[38,39] and are substantiated by prior studies, which suggest lower nailfold capillary density and more avascular zones in patients with POAG compared with controls.[26,48] Therefore, we believe that nailfold capillary abnormalities indicate systemic vascular pathology in POAG. Moreover, these systemic findings are present with ophthalmic microvasculature abnormalities in the same cohort of participants, despite structural differences between the two systems.[49] Retinal arteries lose their internal elastic lamina as they bifurcate at the optic disc and have a thicker muscularis as a compensatory mechanism, a characteristic that differentiates them from arteries of other tissues.[50] In addition, endothelial cells of the retinal arteries are not fenestrated and are linked by tight junctions, unlike peripheral vessels.[51] While nailfold capillaries are only supported by pericytes, optic nerve capillaries are supported by both pericytes and astrocyte processes forming the blood–brain barrier.[52] Despite these anatomic differences, our study quantitatively demonstrated the morphologic and hemodynamic alterations in both microvascular beds. This is consistent with a previous study demonstrating a strong association between optic disc hemorrhage and nail bed hemorrhage in patients with glaucoma.[53]

A prior study found that patients with POAG with low ocular blood flow as measured by color Doppler imaging and laser Doppler flowmetry are more likely to have nailfold capillary vasospasm in response to low temperature compared to patients with POAG with high ocular blood flow values.[54] Additionally, Mozaffarieh et al.[28] used laser Doppler flowmetry to demonstrate that ONH blood flow correlated with finger blood flow measured by nailfold capillary vasospastic response in patients with POAG. A recent study investigated the relationship between nailfold capillary abnormalities and retinal VD in patients with POAG and primary angle closure glaucoma using logistic regression analysis and found nailfold capillary abnormalities, such as lower capillary density, greater tortuosity, and more avascular zones, in these patients compared with controls.[48] All three studies suggest potential correlation between these two vascular systems, but none quantified and correlated the function of both microvascular systems. Our study directly quantified VD and flow in both microvascular beds and demonstrated positive correlations between the two vascular systems in the same cohort of participants. Although the correlations were not significant in the POAG group, which may be due to the small sample size or differences in primary vascular dysregulation among patients with glaucoma,[44] the correlations in the overall cohort suggest a potential common pathway affecting both the ophthalmic and systemic microvascular systems. Furthermore, the correlations between the two systems were present despite the time gap between ophthalmic and nailfold imaging, suggesting that the morphologic alterations observed in patients with POAG are chronic in nature. These data are also consistent with emerging data that the gene variants discovered for POAG are related to vascular elements, and hence one might expect concomitant microvascular changes in both ophthalmic and systemic vascular beds.[55]

On the basis of these findings, we suspect that endothelial dysfunction occurs and persists in patients with POAG, which is supported by previous studies. Polymorphisms in *NOS3* gene are components of gene–environment interactions associated with POAG.[56–58] NOS3 codes for an enzyme responsible

for nitric oxide, which leads to peripheral vasodilation. Reduced number of peripheral circulating endothelial progenitor cells ($CD34^+$ cells), increased levels and sensitivity to endothelin 1, and abnormal response to postural change suggest systemic endothelial dysfunction in patients with glaucoma.[7,59–62] In a large multiethnic meta-analysis of genome-wide association studies, researchers have identified novel risk loci expressed in vascular beds, including vascular endothelial growth factor C and angiopoietin (*ANGPT1*), to be associated with POAG, further highlighting the significance of vascular pathology in these patients.[63] Therefore, multiple facets of endothelial dysfunction may link the alterations in both the ophthalmic and systemic microvascular systems demonstrated in our study, and they suggest a role for treatment targeting the endothelial system in patients with POAG.

There are several limitations to this study. Generalizability may be limited due to the small sample size, predominantly Caucasian population, and exclusion of eyes with high myopia, tilted discs, or previous glaucoma surgeries, which may affect OCTA measurements.[64] Retinal microvasculature can be negatively affected by aging,[65] yet we observed decreased ONH and peripapillary vessel density in patients with POAG, who were younger than controls. Although we tried to address the age difference during recruiting, we ultimately adjusted for age in multivariable analyses. Fourteen percent of participants were excluded due to poor OCTA image quality and motion artifacts. This proportion is consistent with the previously published literature.[66,67] Additionally, although direct communication with the OCTA manufacturer (Topcon) has indicated that IOS is a marker of blood flow, the exact relationship between IOS and blood flow has not been established. Also, large vessel removal of the peripapillary OCTA may not be complete with a semiautomated algorithm, especially if the vessel has relatively low signal intensity compared to its surrounding. This method was chosen over the manual method for standardization and was shown to yield very similar results to the manual method (Supplementary Table S3). Furthermore, the angiogram from Bruch's membrane to 390 µm below was used for OCTA measurements of the deep ONH to include the laminar region[21] but does not fully account for posterior displacement and remodeling of the lamina cribrosa in patients with POAG.[68,69] Improved visualization of the posterior lamina cribrosa surface is needed for better segmentation of the laminar layer and anatomically precise measurement of OCTA signals.[70] Nailfold capillary imaging challenges included inability to automate capillary density and blood flow measurements and variations in time of day or finger temperature during imaging. However, all participants underwent nailfold capillary imaging after their clinic visit to allow for acclimation to their surroundings, and the nailfold imaging was performed in the same room at ambient temperature for standardization. Furthermore, all nailfold capillary measurements were performed by two independent readers masked to disease status. Finally, this study was cross-sectional, so the temporal relationship between pathology in ophthalmic microvasculature and nailfold capillaries cannot be determined. Future prospective longitudinal studies with a larger sample size of patients with POAG are needed to assess for the temporal relationship between these vascular changes and to provide more direct evidence for genetic etiologies.

In summary, this study utilizes SS-OCTA and nailfold capillary microscopy to quantify vascular pathology in both the ophthalmic and nailfold microvascular systems in the same patients with POAG. This study provides novel insight into local and systemic vascular pathology present in POAG and implicates endothelial dysfunction in multiple vascular beds. This study suggests that systemic microvascular pathology is a potential target for treatment of POAG.

Acknowledgments

Supported by the Harvard Glaucoma Center of Excellence, the Miller Research Funds at the Massachusetts Eye and Ear, and the Topcon Research Foundation. M. Wang receives grant funding from NIH K99 EY028631 and R00 EY028631. L.R. Pasquale is supported by NIH NEI EY015473. The funding organizations had no role in the design or conduction of the study; collection, management, analysis, and interpretation of the data; preparation, review, or approval of the manuscript; or decision to submit the manuscript for publication.

Disclosure: **M.K. Shoji**, None; **C.C. Cousins**, None; **C. Saini**, None; **R. Nascimento e Silva**, None; **M. Wang**, None; **S.C. Brauner**, None; **S.H. Greenstein**, None; **L.R. Pasquale**, Bausch & Lomb (C), Verily (C), Twenty-twenty (C), Nicox (C), Skye Bioscience (C), Eyenovia (C); **L.Q. Shen**, Topcon (C)

References

1. Quigley HA, Green WR. The histology of human glaucoma cupping and optic nerve damage: clin-

icopathologic correlation in 21 eyes. *Ophthalmology*. 1979;86(10):1803–1827.
2. Schumann J, Orgül S, Gugleta K, Dubler B, Flammer J. Interocular difference in progression of glaucoma correlates with interocular differences in retrobulbar circulation. *Am J Ophthalmol*. 2000;129(6):728–733.
3. Findl O, Rainer G, Dallinger S, et al. Assessment of optic disk blood flow in patients with open-angle glaucoma. *Am J Ophthalmol*. 2000;130(5):589–596.
4. Grunwald JE, Riva CE, Stone RA, Keates EU, Petrig BL. Retinal autoregulation in open-angle glaucoma. *Ophthalmology*. 1984;91(12):1690–1694.
5. Gherghel D, Hosking SL, Cunliffe IA. Abnormal systemic and ocular Vascular response to temperature provocation in primary open-angle glaucoma patients: a case for autonomic failure? *Invest Ophthalmol Vis Sci*. 2004;45(10):3546–3554.
6. Su WW, Cheng ST, Ho WJ, Tsay PK, Wu SC, Chang SHL. Glaucoma is associated with peripheral vascular endothelial dysfunction. *Ophthalmology*. 2008;115(7):1173–1179.
7. Fadini GP, Pagano C, Baesso I, et al. Reduced endothelial progenitor cells and brachial artery flow-mediated dilation as evidence of endothelial dysfunction in ocular hypertension and primary open-angle glaucoma. *Acta Ophthalmol*. 2010;88(1):135–141.
8. Birinci H, Danaci M, Öge I, Erkan ND. Ocular blood flow in healthy and primary open-angle glaucomatous eyes. *Ophthalmologica*. 2002;216(6):434–437.
9. Galassi F, Nuzzaci G, Sodi A, Casi P, Cappelli S, Vielmo A. Possible correlations of ocular blood flow parameters with intraocular pressure and visual-field alterations in glaucoma: a study by means of color doppler imaging. *Ophthalmologica*. 1994;208(6):304–308.
10. Feke GT, Pasquale LR. Retinal blood flow response to posture change in glaucoma patients compared with healthy subjects. *Ophthalmology*. 2008;115(2):246–252.
11. Feke GT. Laser based instruments for ocular blood flow assessment. *J Biomed Opt*. 1998;3(4):415–422.
12. Kaiser HJ, Schoetzau A, Stumpfig D, Flammer J. Blood-flow velocities of the extraocular vessels in patients with high- tension and normal-tension primary open-angle glaucoma. *Am J Ophthalmol*. 1997;123(3):320–327.
13. Gherghel D, Orgül S, Gugleta K, Flammer J. Retrobulbar blood flow in glaucoma patients with nocturnal over-dipping in systemic blood pressure. *Am J Ophthalmol*. 2001;132(5):641–647.
14. Gherghel D, Orgül S, Gugleta K, Gekkieva M, Flammer J. Relationship between ocular perfusion pressure and retrobulbar blood flow in patients with glaucoma with progressive damage. *Am J Ophthalmol*. 2000;130(5):597–605.
15. Akil H, Huang AS, Francis BA, Sadda SR, Chopra V. Retinal vessel density from optical coherence tomography angiography to differentiate early glaucoma, pre-perimetric glaucoma and normal eyes. *PLoS One*. 2017;12(2):1–12.
16. Lévêque PM, Zéboulon P, Brasnu E, Baudouin C, Labbé A. Optic disc vascularization in glaucoma: value of spectral-domain optical coherence tomography angiography. *J Ophthalmol*. 2016;2016:6956717.
17. Liu L, Jia Y, Takusagawa HL, et al. Optical coherence tomography angiography of the peripapillary retina in glaucoma. *JAMA Ophthalmol*. 2015;133(9):1045–1052.
18. Yarmohammadi A, Zangwill LM, Diniz-Filho A, et al. Optical coherence tomography angiography vessel density in healthy, glaucoma suspect, and glaucoma eyes. *Invest Ophthalmol Vis Sci*. 2016;57(9):OCT451–OCT459.
19. Potsaid B, Baumann B, Huang D, et al. Ultrahigh speed 1050nm swept source/Fourier domain OCT retinal and anterior segment imaging at 100,000 to 400,000 axial scans per second. *Opt Express*. 2010;18(19):20029–20048.
20. Stanga PE, Tsamis E, Papayannis A, Stringa F, Cole T, Jalil A. Swept-source optical coherence tomography Angio^{TM} (Topcon Corp, Japan): technology review. *Dev Ophthalmol*. 2016;56:13–17.
21. Nascimento e Silva R, Chiou CA, Wang M, et al. Microvasculature of the optic nerve head and peripapillary region in patients with primary open-angle glaucoma. *J Glaucoma*. 2019;28(4):281–288.
22. Nascimento e Silva R, Chiou CA, Wang M, et al. Quantification of the peripapillary microvasculature in eyes with glaucomatous paracentral visual field loss. *Ophthalmol Glaucoma*. 2021;4(3):286–294.
23. Etehad Tavakol M, Fatemi A, Karbalaie A, Emrani Z, Erlandsson B-E. Nailfold capillaroscopy in rheumatic diseases: which parameters should be evaluated? *Biomed Res Int*. 2015;2015:974530.
24. Chandrasekera E, An D, McAllister IL, Yu DY, Balaratnasingam C. Three-dimensional microscopy demonstrates series and parallel organization of human peripapillary capillary plexuses. *Invest Ophthalmol Vis Sci*. 2018;59(11):4327–4344.

25. Gasser P, Flammer J. Blood-cell velocity in the nailfold capillaries of patients with normal-tension and high-tension glaucoma. *Am J Ophthalmol*. 1991;111(5):585–588.
26. Pasquale LR, Hanyuda A, Ren A, et al. Nailfold capillary abnormalities in primary open-angle glaucoma: a multisite study. *Invest Ophthalmol Vis Sci*. 2015;56(12):7021–7028.
27. Kosior-Jarecka E, Bartosińska J, Łukasik U, et al. Results of nailfold capillaroscopy in patients with normal-tension glaucoma. *Curr Eye Res*. 2018;43(6):747–753.
28. Mozaffarieh M, Osusky R, Schötzau A, Flammer J. Relationship between optic nerve head and finger blood flow. *Eur J Ophthalmol*. 2010;20(1):136–141.
29. Gasser P, Orgul S, Dubler B, Bucheli B, Flammer J. Relation between blood flow velocities in the ophthalmic artery and in nailfold capillaries. *Br J Ophthalmol*. 1999;83(4):505.
30. Jonas JB, Kling F, Grundler AE. Optic disc shape, corneal astigmatism, and amblyopia. *Ophthalmology*. 1997;104(11):1934–1937.
31. Vongphanit J, Mitchell P, Wang JJ. Population prevalence of tilted optic disks and the relationship of this sign to refractive error. *Am J Ophthalmol*. 2002;133(5):679–685.
32. Cortes S, Cutolo M. Capillarosecopic patterns in rheumatic diseases. *Acta Reumatol Port*. 2007;32(1):29–36.
33. Cousins CC, Chou JC, Greenstein SH, et al. Resting nailfold capillary blood flow in primary open-angle glaucoma. *Br J Ophthalmol*. 2019;103(2):203–207.
34. Sun Z, Tang F, Wong R, et al. OCT angiography metrics predict progression of diabetic retinopathy and development of diabetic macular edema: a prospective study. *Ophthalmology*. 2019;126(12):1675–1684.
35. Chen HSL, Liu CH, Wu WC, Tseng HJ, Lee YS. Optical coherence tomography angiography of the superficial microvasculature in the macular and peripapillary areas in glaucomatous and healthy eyes. *Invest Ophthalmol Vis Sci*. 2017;58(9):3637–3645.
36. Rao HL, Pradhan ZS, Weinreb RN, et al. Regional comparisons of optical coherence tomography angiography vessel density in primary open-angle glaucoma. *Am J Ophthalmol*. 2016;171:75–83.
37. Cutolo M, Grassi W, Cerinic MM. Raynaud's phenomenon and the role of capillaroscopy. *Arthritis Rheum*. 2003;48(11):3023–3030.
38. Emrani Z, Karbalaie A, Fatemi A, Etehadtavakol M, Erlandsson BE. Capillary density: an important parameter in nailfold capillaroscopy. *Microvasc Res*. 2017;109:7–18.
39. Hofstee HMA, Serné EH, Roberts C, et al. A multicentre study on the reliability of qualitative and quantitative nail-fold videocapillaroscopy assessment. *Rheumatology*. 2012;51(4):749–755.
40. Mugii N, Hasegawa M, Hamaguchi Y, et al. Reduced red blood cell velocity in nail-fold capillaries as a sensitive and specific indicator of microcirculation injury in systemic sclerosis. *Rheumatology*. 2009;48(6):696–703.
41. Glickman ME, Rao SR, Schultz MR. False discovery rate control is a recommended alternative to Bonferroni-type adjustments in health studies. *J Clin Epidemiol*. 2014;67(8):850–857.
42. Richter GM, Sylvester B, Chu Z, et al. Peripapillary microvasculature in the retinal nerve fiber layer in glaucoma by optical coherence tomography angiography: focal structural and functional correlations and diagnostic performance. *Clin Ophthalmol*. 2018;12:2285–2296.
43. Shin JW, Lee J, Kwon J, Choi J, Kook MS. Regional vascular density-visual field sensitivity relationship in glaucoma according to disease severity. *Br J Ophthalmol*. 2017;101(12):1666–1672.
44. Flammer J, Konieczka K, Flammer AJ. The primary vascular dysregulation syndrome: implications for eye diseases. *EPMA J*. 2013;4(1):14.
45. Hayreh SS. Pathophysiology of glaucomatous optic neuropathy: role of optic nerve head vascular insufficiency. *Curr J Glaucoma Pract*. 2008;2:6–17.
46. Zeitz O, Galambos P, Wagenfeld L, et al. Glaucoma progression is associated with decreased blood flow velocities in the short posterior ciliary artery. *Br J Ophthalmol*. 2006;90(10):1245–1248.
47. Pinto LA, Vandewalle E, Stalmans I. Disturbed correlation between arterial resistance and pulsatility in glaucoma patients. *Acta Ophthalmol*. 2012;90(3):e214–e220.
48. Rong X, Cai Y, Li M, Chen X, Kang L, Yang L. Relationship between nailfold capillary morphology and retinal thickness and retinal vessel density in primary open-angle and angle-closure glaucoma. *Acta Ophthalmol*. 2020;98(7):e882–e887.
49. Flammer J, Konieczka K, Bruno RM, Virdis A, Flammer AJ, Taddei S. The eye and the heart. *Eur Heart J*. 2013;34(17):1270–1278.
50. Anand-Apte B, Hollyfield JG. Developmental anatomy of the retinal and choroidal vasculature. In: Joseph B., Barbara B., David B., Reza D., Peter B., Paul B., Dean B., Patricia D'Amore, Henry E., Linda M., Jerry N., Thomas R., Ernst T. Editor

in Chief: Darlene Dartt. *Encyclopedia of the Eye*. Cambridge, MA, USA: Elsevier; 2010:9–15.
51. Shakib M, Cunha-Vaz JG. Studies on the permeability of the blood-retinal barrier, IV: junctional complexes of the retinal vessels and their role in the permeability of the blood-retinal barrier. *Exp Eye Res*. 1966;5(3):229–234.
52. Kim JH, Jin HK, Jeong AP, et al. Blood-neural barrier: intercellular communication at glio-vascular interface. *J Biochem Mol Biol*. 2006;39(4):339–345.
53. Park H-YL, Park S-H, Oh Y-S, Park CK. Nail bed hemorrhage: a clinical marker of optic disc hemorrhage in patients with glaucoma. *Arch Ophthalmol (Chicago, Ill 1960)*. 2011;129(10):1299–1304.
54. Emre M, Orgül S, Gugleta K, Flammer J. Ocular blood flow alteration in glaucoma is related to systemic vascular dysregulation. *Br J Ophthalmol*. 2004;88(5):662–666.
55. Gharahkhani P, Jorgenson E, Hysi P, et al. Genome-wide meta-analysis identifies 127 open-angle glaucoma loci with consistent effect across ancestries. *Nat Commun*. 2021;12(1):1258.
56. Kang JH, Wiggs JL, Rosner BA, et al. Endothelial nitric oxide synthase gene variants and primary open-angle glaucoma: interactions with sex and postmenopausal hormone use. *Invest Ophthalmol Vis Sci*. 2010;51(2):971–979.
57. Kang JH, Wiggs JL, Haines J, Abdrabou W, Pasquale LR. Reproductive factors and NOS3 variant interactions in primary open-angle glaucoma. *Mol Vis*. 2011;17:2544–2551.
58. Kang JH, Wiggs JL, Rosner BA, Haines J, Abdrabou W, Pasquale LR. Endothelial nitric oxide synthase gene variants and primary open-angle glaucoma: interactions with hypertension, alcohol intake, and cigarette smoking. *Arch Ophthalmol*. 2011;129(6):773–780.
59. Clark CV, Mapstone R. Systemic autonomic neuropathy in open-angle glaucoma. *Doc Ophthalmol*. 1987;64(2):179–185.
60. Buckley C, Hadoke PWF, Henry E, O'Brien C. Systemic vascular endothelial cell dysfunction in normal pressure glaucoma. *Br J Ophthalmol*. 2002;86(2):227–232.
61. Sugiyama T, Moriya S, Oku H, Azuma I. Association of endothelin-1 with normal tension glaucoma: clinical and fundamental studies. *Surv Ophthalmol*. 1995;39(suppl 1):S49–S56.
62. Kaiser HJ, Flammer J, Wenk M, Lüscher T. Endothelin-1 plasma levels in normal-tension glaucoma: abnormal response to postural changes. *Graefes Arch Clin Exp Ophthalmol*. 1995;233(8):484–488.
63. Craig JE, Han X, Qassim A, et al. Multitrait analysis of glaucoma identifies new risk loci and enables polygenic prediction of disease susceptibility and progression. *Nat Genet*. 2020;52(2):160–166.
64. In JH, Lee SY, Cho SH, Hong YJ. Peripapillary vessel density reversal after trabeculectomy in glaucoma. *J Ophthalmol*. 2018;2018:8909714.
65. Wei Y, Jiang H, Shi Y, et al. Age-related alterations in the retinal microvasculature, microcirculation, and microstructure. *Invest Ophthalmol Vis Sci*. 2017;58(9):3804–3817.
66. Akagi T, Iida Y, Nakanishi H, et al. Microvascular density in glaucomatous eyes with hemifield visual field defects: an optical coherence tomography angiography study. *Am J Ophthalmol*. 2016;168:237–249.
67. Ghasemi Falavarjani K, Al-Sheikh M, Akil H, Sadda SR. Image artefacts in swept-source optical coherence tomography angiography. *Br J Ophthalmol*. 2017;101(5):564–568.
68. Park SC, Brumm J, Furlanetto RL, et al. Lamina cribrosa depth in different stages of glaucoma. *Invest Ophthalmol Vis Sci*. 2015;56(3):2059–2064.
69. Kim DW, Jeoung JW, Kim YW, et al. Prelamina and lamina cribrosa in glaucoma patients with unilateral visual field loss. *Invest Ophthalmol Vis Sci*. 2016;57(4):1662–1670.
70. Girard MJA, Tun TA, Husain R, et al. Lamina cribrosa visibility using optical coherence tomography: comparison of devices and effects of image enhancement techniques. *Invest Ophthalmol Vis Sci*. 2015;56(2):865–874.